Check for updates

Deformation structural style of the rioni foreland fold-and-thrust belt, western greater caucasus: Insight from the balanced cross-section

Victor Alania[1]*, George Melikadze[1], Paolo Pace[2,3], István Fórizs[4,5], Tamar Beridze[6], Onise Enukidze[1], Anzor Giorgadze[7] and Alexander Razmadze[1]

[1]Institute of Geophysics, I. Javakhishvili Tbilisi State University, Tbilisi, Georgia, [2]Department of Engineering and Geology, "G. d'Annunzio" University of Chieti-Pescara, Chieti, Italy, [3]PACE Geoscience, Chieti, Italy, [4]Institute for Geological and Geochemical Research, Research Centre for Astronomy and Earth Sciences, ELKH, Budapest, Hungary, [5]CSFK, MTA Centre of Excellence, Budapest, Hungary, [6]A. Janelidze Institute of Geology, I. Javakhishvili Tbilisi State University, Tbilisi, Georgia, [7]Faculty of Mining and Geology, Georgian Technical University, Tbilisi, Georgia

The Rioni foreland fold-and-thrust belt is part of the Greater Caucasus pro-wedge and is one of the most important examples of the collision-driven far-field deformation of the Arabia-Eurasia convergence zone. Here we show the deformation structural style of the Rioni foreland fold-and-thrust belt based on seismic reflection profiles and regional balanced cross-section. The main style of deformation within the Rioni foreland fold-and-thrust belt is represented by a set of fault-propagation folds, duplexes, and triangle zone. The regional balanced cross-section shows that fault-propagation folds above the upper detachment level can develop by piggyback and break-back thrust sequences. Formation of fault-bend fold duplex structures above the lower detachment is related to piggyback thrust sequences. A balanced section restoration of compressional structures across the Rioni foreland fold-and-thrust belt provides a minimum estimate of shortening of −40%, equivalent −42.78 km. The synclines within the Rioni foreland fold-and-thrust belt are filled by the Middle Miocene-Pleistocene shallow marine and continental syn-tectonic sediments, forming a series of typical thrust-top basins. Fault-propagation folds and duplex structures formed the main structure of the thrust-top basin. The evolution of the thrust-top basins was mainly controlled by the kinematics of thrust sequences. Using end-member modes of thrust sequences, the thrust-top basins are divided into: 1) Type I-piggyback basin, 2) Type II-break-back basin, and 3) Type III—formation of thrust-top basin characterized by bi-vergent geometry and related to combined, piggyback and piggyback back thrust sequences.
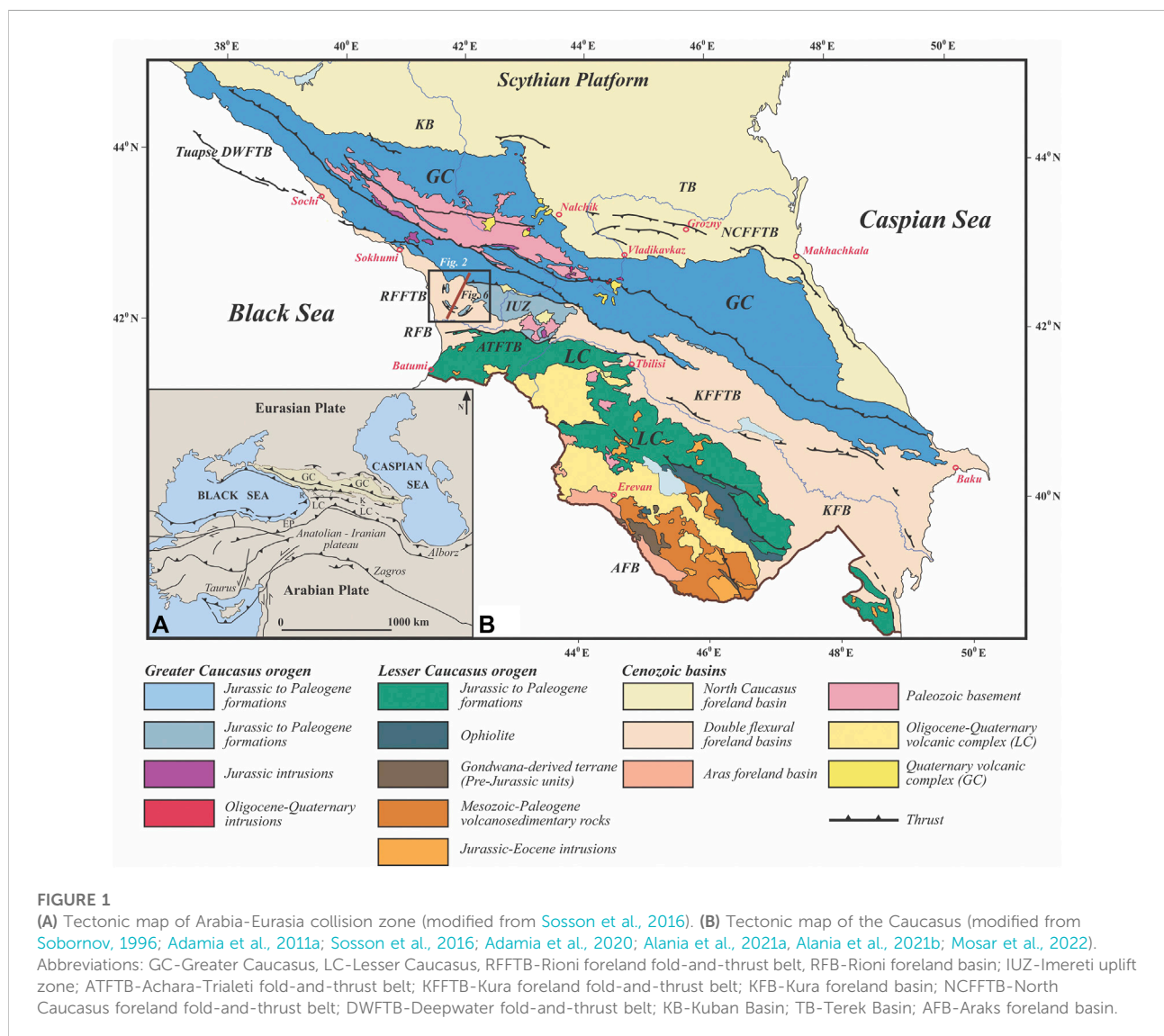
Introduction

An understanding of the structural architecture of the
foreland fold-and-thrust belts is important in the application
of this knowledge to the compressional deformation history of
orogens. In a foreland basin system, the frontal part of the
orogenic wedge sediments is deformed into a series of fault-
related folds and associated thrust-top basins (e.g., DeCelles and
Giles, 1996; Roure, 2008). The timing of thrust-top basins
sedimentation in the foreland basin is important because it is
one of the indicators for the timing of shortening, and uplift of

the orogens; syn-tectonic deposition within the basin records the
upward stratigraphic evolution during the deformation (e.g., Ori
and Friend, 1984; Turner, 1988; Suppe et al., 1992; Butler and
Grasso, 1993; DeCelles and Giles, 1996; Suriano et al., 2015;
Chanvry et al., 2018; Heydarzadeh et al., 2020).

The Rioni foreland fold-and-thrust belt (RFFTB) is one of
the most important examples of the collision-driven far-field
deformation of the Arabia-Eurasia convergence zone
(Figure 1A). The RFFTB is a part of the Greater Caucasus
pro-wedge (Alania et al., 2021a) and is one of the main
hydrothermal provinces of west Georgia (Melikadze et al.,

FIGURE 1
(A) Tectonic map of Arabia-Eurasia collision zone (modified from Sosson et al., 2016). **(B)** Tectonic map of the Caucasus (modified from
Sobornov, 1996; Adamia et al., 2011a; Sosson et al., 2016; Adamia et al., 2020; Alania et al., 2021a, Alania et al., 2021b; Mosar et al., 2022).
Abbreviations: GC-Greater Caucasus, LC-Lesser Caucasus, RFFTB-Rioni foreland fold-and-thrust belt, RFB-Rioni foreland basin; IUZ-Imereti uplift
zone; ATFTB-Achara-Trialeti fold-and-thrust belt; KFFTB-Kura foreland fold-and-thrust belt; KFB-Kura foreland basin; NCFFTB-North
Caucasus foreland fold-and-thrust belt; DWFTB-Deepwater fold-and-thrust belt; KB-Kuban Basin; TB-Terek Basin; AFB-Araks foreland basin.

FIGURE 2
Geological map of RFFTB and surrounding area (modified from Janelidze and Kandelaki, 1956; Vakhania, 2008a, Vakhania, 2008b; Adamia et al., 2020). Abbreviations: RFFTB, Rioni foreland fold-and-thrust belt; SSGC, Southern Slope of Greater Caucasus; CSA, Chaladidi-Sagvamischao anticline; KVA, Kvaloni anticline; KA, Khobi anticline; SA-Senaki anticline; NOA, Nokhalakhevi anticline; TSA, Tsaishi anticline; SHA, Sashurgaio anticline; ZUA, Zugdidi anticline; STA, Satanjo anticline; SBA, Saberios anticline; SAA, Sarakoni anticline.
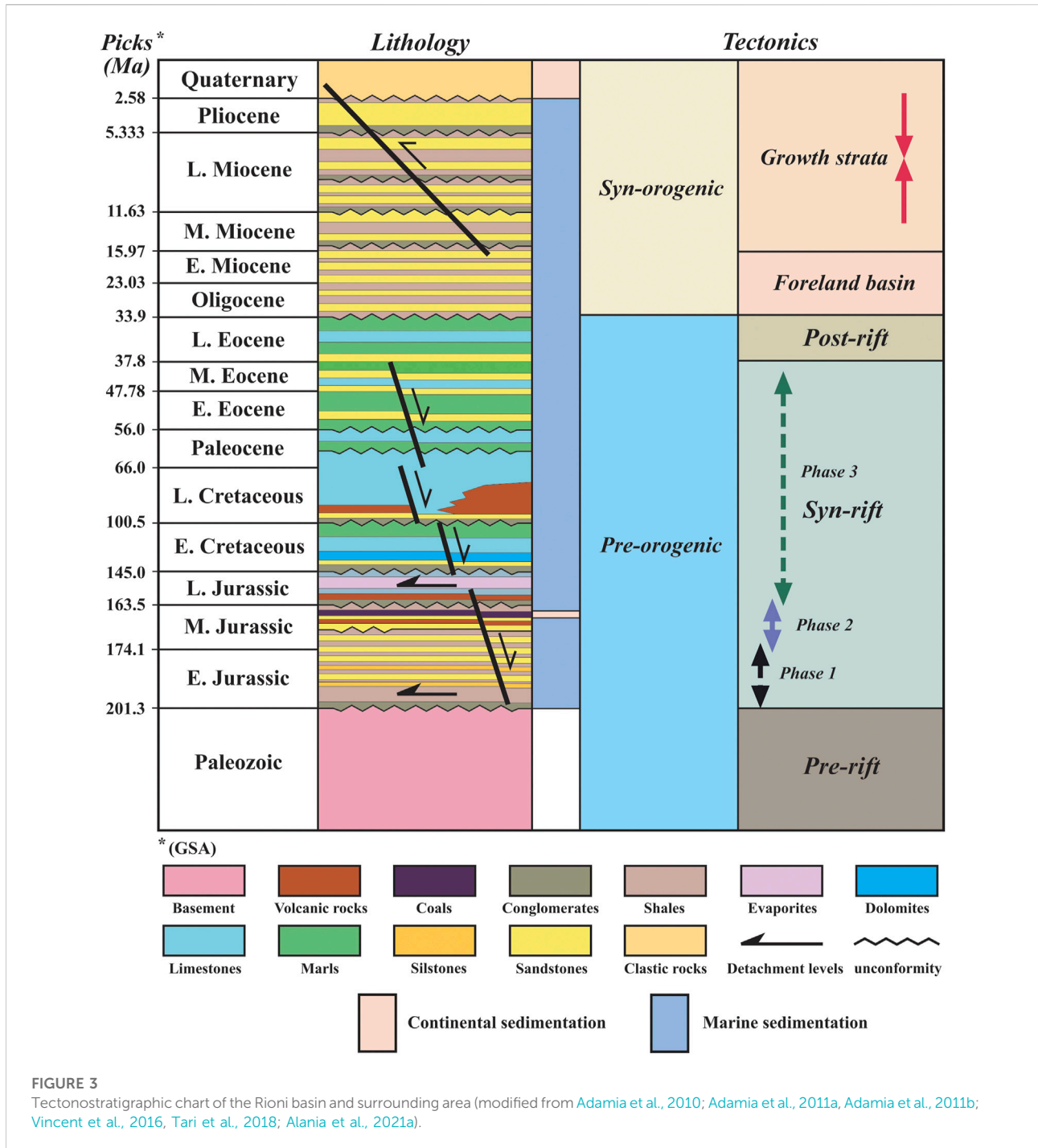
2014). During the last several years the understanding of the structure and kinematic evolution of the RFFTB has changed to a great extent. These studies have investigated this region focusing on 1) the tectonic development of the RFFTB (e.g., Banks et al., 1997; Vakhania, 2008a; Vakhania, 2008b; Adamia et al., 2010; Forte et al., 2014; Cowgill et al., 2016; Tibaldi et al., 2018; Alania et al., 2021a; Trexler et al., 2022), 2) the deformation style of the RFFTB (e.g., Banks et al., 1997; Cowgill et al., 2016; Tibaldi et al., 2017a; Tibaldi et al., 2017b; Tari et al., 2018; Tibaldi et al., 2018), 3) the timing of deformation of the RFFTB (e.g., Banks et al., 1997; Cowgill et al., 2016; Tari et al., 2018; Trexler et al., 2020; Alania et al., 2021a), and 4) the active structures of the RFFTB (e.g., Tsereteli et al., 2016; Adamia et al., 2017; Tibaldi et al., 2017a; Tibaldi et al., 2017b; Tibaldi et al., 2020; Trexler et al., 2020).

Although previous studies have achieved an understanding of the role of detachments in the formation of the series of fault-related folds in the thin-skinned RFFTB, they are mainly dependent on boreholes data and field outcrops studies. Therefore, the deformation structural styles of this foreland fold-and-thrust belt have still remained controversial.

The main goals of this study are 1) to determine the deformation structural style, 2) to calculate the shortening by comparing the regional balanced and restored cross-sections, and 3) to determine the types of thrust-top basins using thrust sequences models. For these purposes, regional balanced and restored cross-sections were constructed across the Rioni foreland fold-and-thrust belt, based on surface and sub-surface data (seismic profiles and well data).

Geological setting

The Rioni foreland basin system is located between the Lesser Caucasus (LC) and the Greater Caucasus (GC) orogens (Figures 1A,B, 2). Deformation of the Rioni double flexural foreland basin (Banks et al., 1997) was controlled by the action of two opposing orogenic fronts, the LC retro-wedge to the south and the GC pro-wedge to the north (Alania et al., 2021a). The tectonic evolution of LC and GC is the result of the Arabia-Eurasia collision during Alpine times, which led to the inversion of back-arc basins and the formation of two

FIGURE 3
Tectonostratigraphic chart of the Rioni basin and surrounding area (modified from Adamia et al., 2010; Adamia et al., 2011a, Adamia et al., 2011b; Vincent et al., 2016, Tari et al., 2018; Alania et al., 2021a).

orogens with the Rioni and Kura foreland basins in between (Figure 1B) (e.g., Adamia et al., 1981; Sobornov, 1996; Banks et al., 1997; Mosar et al., 2010; Nemcok et al., 2013; Cowgill et al., 2016; Sosson et al., 2016; Tari et al., 2018; Alania et al., 2021a; Alania et al., 2021b; Alania et al., 2021c; Corrado et al., 2021; Gusmeo et al., 2021; Gusmeo et al., 2022; Tari et al., 2021; Cowgill et al., 2022; Mosar et al., 2022). The Rioni and

Kura foreland basins in turn are divided from each other by the Imereti Uplift Zone (IUZ) (Figure 1B).

Foreland basin sedimentation in the Rioni Basin, as well as in the Kura foreland basin is regarded to have started during the Oligocene to Early Miocene, consistent with the onset of rapid subsidence from the south by LC and from the north by GC (Alania et al., 2017; Alania et al., 2021a). North and central parts

of the Rioni foreland basin during the Middle Miocene-Pleistocene time were deformed and shortening is concentrated at the outer part of the GC pro-wedge (Alania et al., 2021a). A similar picture can be observed in the Kura foreland fold-and-thrust belt (KFFTB), where compressional deformation began in the Middle Miocene (Alania et al., 2017; Corrado et al., 2021; Gusmeo et al., 2021).

The RFFTB sedimentary infill (more than 7 km) consists of pre-and syn-orogenic sequences. The simplified geological evolution of the studied area is summarized in a tectonostratigraphic chart (Figure 3). The pre-Mesozoic basement of the RFFTB exposed in the IUZ (Figure 1B) comprises Hercynian granitic metamorphic rocks in its core, overlain by Devonian to Carboniferous phyllites (Adamia et al., 2011a). The basement of the RFFTB is in general tilting towards the north and the associated orogenic flexure of the foreland region (Banks et al., 1997). Most of the pre-Mesozoic basement is intruded by granitoid and covered with volcanogenic rocks of the Middle Jurassic age (Adamia et al., 2011a).

The pre-orogenic sequences consist of Jurassic-Late Eocene shallow and deep marine deposits (e.g., Tari et al., 2018). According to Vincent et al. (2016) within the GC back-arc basin are distinguished three main phases of extension: 1) the first phase started in the Sinemurian (Early Jurassic); 2) a main phase of extension took place from the Aalenian to the Bajocian (Middle Jurassic); and 3) a thermal-sagging phase from the Bathonian (Middle Jurassic) to the Eocene. The Early Jurassic sandstones and shales (about 1500 m thick) are exposed north and south of RFFTB. Middle Jurassic is represented by Bajocian debris flow deposits and turbidities with rare intercalations of calk-alkaline andesite-basalts and the Bathonian freshwater-lacustrine coal-bearing sandy-argillaceous rocks; thickness is about 2500 m. Late Jurassic is represented by evaporites, clastic rocks, and basalts (about 500 m thick). Early Cretaceous turbidities, dolomites, limestones, and marls, with conglomerates at the base, transgressively rest on Late Jurassic rocks; thickness is about 350–400 m (e.g., Adamia et al., 2011a; Adamia et al., 2011b). The Late Aptian, Albian, and Cenomanian sequence is dominated by siliciclastic rocks. Late Cretaceous, Paleocene, and Eocene deposits are mainly built up by mixed carbonate-siliciclastic-volcaniclastic rocks; their thickness in some places exceeds 2000m (e.g., Adamia et al., 2011a).

The syn-orogenic sequences are composed of the foreland basin (Oligocene-Early Miocene) and syn-tectonic strata (Alania et al., 2021a). The Oligocene-Neogene stratigraphy of the RFFTB is dominated by siliciclastic sequences. The Oligocene-Early Miocene is represented mainly by the alternation of shales and sandstones and is underlain unconformably by the marl-dominated Eocene sequence; their thickness is about 800–900 m (Mayer et al., 2018; Sachsenhofer et al., 2018; Tari et al., 2018). Syn-tectonic strata of Middle-Late Miocene, Pliocene, and Pleistocene are represented by shallow marine and continental, predominantly terrigenous clastic rocks. The
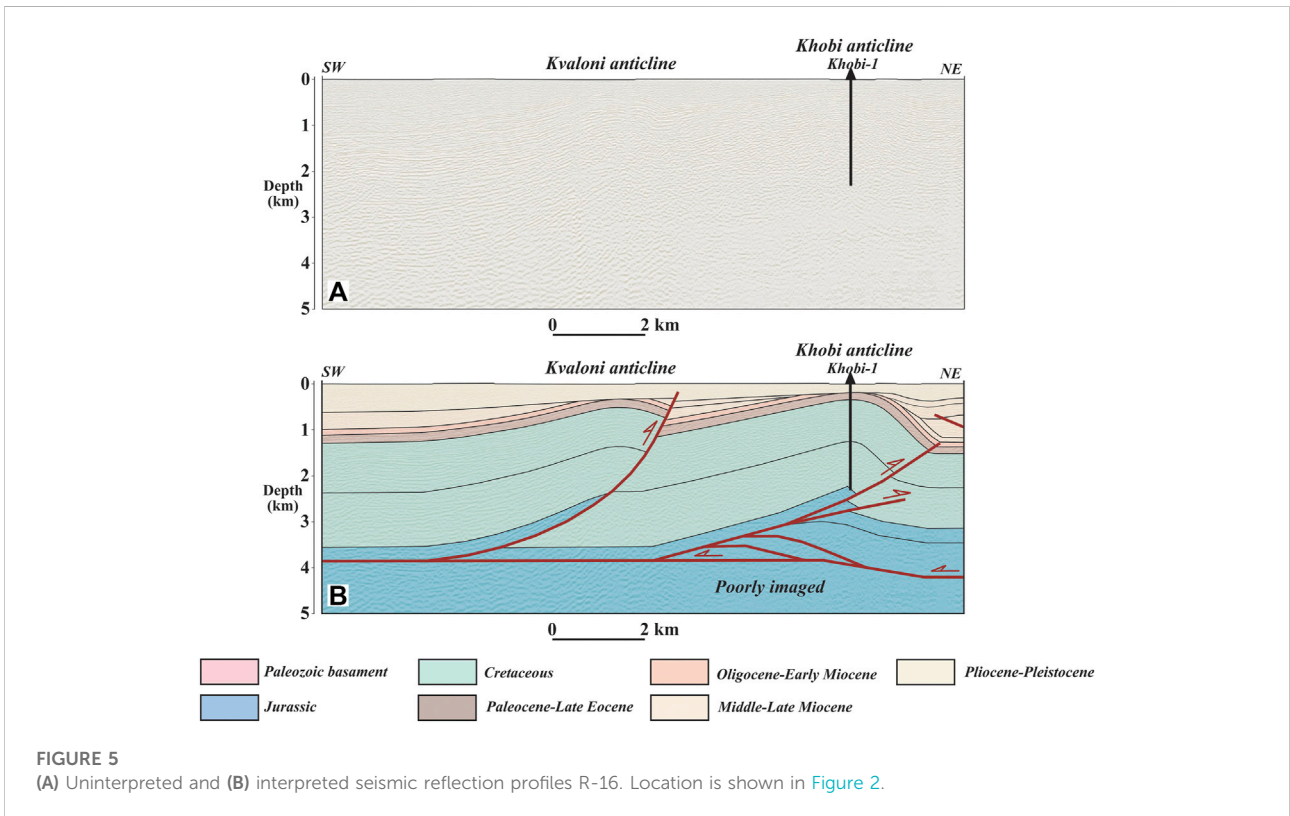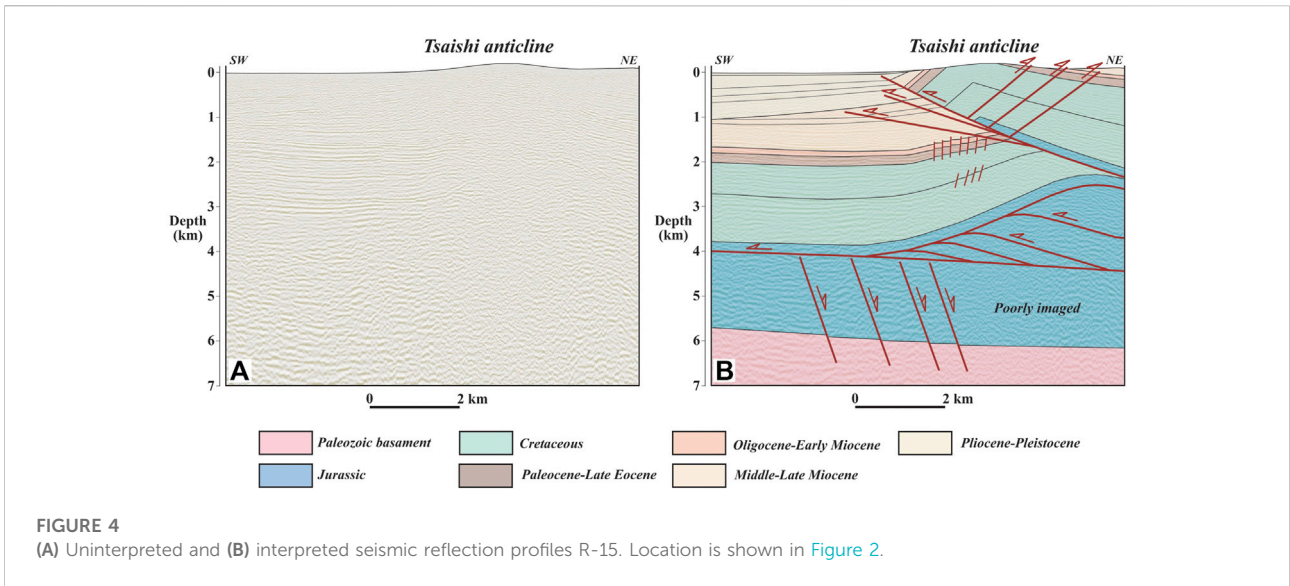
thickness of the syn-tectonic strata is about 1,500–2000 m (e.g., Adamia et al., 2010; Tari et al., 2018; Alania et al., 2021a). The Holocene is represented by undifferentiated continental strata and river-bed alluvial deposits (e.g., Adamia et al., 2010).

The RFFTB underwent from the Middle Miocene—Pleistocene N- to S-directed shortening (Banks et al., 1997; Tibaldi et al., 2017a; Tibaldi et al., 2017b; Tari et al., 2018; Alania et al., 2021a). The characteristic structural styles are represented by fault-related folds detached along the basal thrust which soles within the Late Jurassic evaporates and are dominated by a thin-skinned tectonic style (Banks et al., 1997; Adamia et al., 2010; Forte et al., 2014; Cowgill et al., 2016; Adamia et al., 2017; Tibaldi et al., 2017a; Tibaldi et al., 2017b; Tari et al., 2018; Alania et al., 2021). The RFFTB system consists of several major anticlines, which from south to north are the Chaladidi-Sagvamichao, Kvaloni, Khobi, Tsaishi, Senaki, Nokalakevi, Sashurgaio, Zugdidi, Satanjo, Saberios, and Sarakoni anticlines. South of the Tsaishi anticline, the Chaladidi-Sagvamichao, Kvaloni, and Khobi anticlines have no evident expression at the surface and it has been imaged by seismic and boreholes data (Vakhania, 2008a; Vakhania, 2008b; Tari et al., 2018). The Tsaishi anticline is the fold with the deepest level of exhumation in the study area, and as a result, the Late Cretaceous limestones crop out in its core (e.g., Banks et al., 1997; Tibaldi et al., 2017a; Tibaldi et al., 2017b; Tari et al., 2018). Curve-shaped thrusts are developed north of the frontal folds of the RFFTB (Figure 2). According to Tibaldi et al. (2018), the structural development of the arcuate thrust system within RFFTB is related to oblique, asymmetric indentation of an upper crustal block moving to the SSW.

Recent GPS and earthquake data indicate that the RFFTB is still tectonically active and the earthquakes focal mechanisms are mainly thrust faults (e.g., Adamia et al., 2004; Tsereteli et al., 2016, Adamia et al., 2017; Sokhadze et al., 2018; Tibaldi et al., 2020, Tibaldi et al., 2021).

Data and methods

The database consists of published and unpublished data as well as field observations. The surface geological information is obtained from 1:100,000 and 1: 200,000 geological maps (Janelidze and Kandelaki, 1956; Adamia et al., 2020) of the study area (Figure 2) and relevant papers (Banks et al., 1997; Adamia et al., 2010; Adamia et al., 2017; Tibaldi et al., 2017a; Tibaldi et al., 2017b; Tari et al., 2018; Adamia et al., 2020; Alania et al., 2021a). Fault-related folding and wedge thrust folding theories (Medwedeff, 1990; Suppe and Medwedeff, 1990; Shaw et al., 2005; Jabbour et al., 2012; Brandes and Tanner, 2014) were used in the interpretation of 2D depth-migrated seismic

FIGURE 4
(A) Uninterpreted and **(B)** interpreted seismic reflection profiles R-15. Location is shown in Figure 2.

FIGURE 5
(A) Uninterpreted and **(B)** interpreted seismic reflection profiles R-16. Location is shown in Figure 2.

reflection profiles (R-15, R-16) (Figures 4A, 5A) and construction of the regional balanced and restored cross-sections (A-A¹) across RFFTB (Figures 6A,B). The balanced cross-section is approximately parallel to the thrust transport direction and has a total length of 64 km. Interpretation of 2D

seismic reflection profiles and constraints on balanced cross-section geometry comprise structural information (position of stratigraphic contacts, faults, thrusts, dips) and thicknesses of lithostratigraphic units. For interpretation of 2D depth-migrated seismic profiles, construction of regional balanced

FIGURE 6
(A) Balanced—A-A¹ and **(B)** restored cross-sections. Location is shown in Figures 1, 2. Abbreviations: T1-T7—Thrusts; D1, D2, Detachments; CSA, Chaladidi-Sagvamischao anticline; SB, Sagvamischao basin; KVA, Kvaloni anticline; TB, Teklati basin; KA, Khobi anticline; KB, Khobi basin; NOA, Nokhalakhevi anticline; NOB, Nokhalakevi Basin; TSA, Tsaishi anticline; NB, Narazeni basin; SHA, Sashurgaio anticline; DZB, Dikhazungi basin; SAA, Sarakoni anticline; TSB-Tsalenjikha basin.

and restored cross-sections and forward kinematic modeling was used the Move 2018.2 software (2018–2019 academic licenses from Midland Valley). Balancing and restorations were performed using Move structural modeling software based on bed length and thickness conservation and the built-in flexural-slip algorithm for the sedimentary cover. Two kinematic algorithms were used during the construction of the forward kinematic model: 1) fault-propagation fold, and 2) fault-bend fold.

Results

We obtained four 2D depth-migrated seismic profiles (R-15, and R-16) through the Tsaishi, Kvaloni, and Khobi anticlines (Figures 4, 5) and cover the central part of the RFFTB (Figure 2). Strata boundaries on seismic profiles are constrained by geologic maps and well data. The geometry of faults within the central part of the RFFTB can be interpreted through direct fault-plane reflection and truncation of seismic reflections. The seismic profile R-15 (Figures 4A,B) clearly illustrate the geometry of the Tsaishi anticline. Interpreted seismic profile show that the Tsaishi anticline is a south-vergent fault-propagation fold whose front limb is broken by thrust faults. The backlimb of the Tsaishi anticline is complicated by backthrusts (Figure 4B). The top section is represented by Tertiary, Cretaceous, and Late Jurassic strata. The Base of the section is marked by the upper detachment, which correlates to the evaporates of the Late Jurassic. The lower section is represented by duplexes and is composed of Early-Middle Jurassic rocks (Figure 4B).

The seismic reflection profile R-16 (Figures 5A,B) revealed the geometry of Kvaloni and Khobi anticlines and show that these anticlines are north-vergent fault-propagation folds. Duplexes made-up by Middle Jurassic rocks are developed under the Khobi anticline (Figure 5B). The growth strata geometry within the seismic profile is well imaged and shows onlaps and fanning limb dips of Khobi fold. Growth strata above Kvaloni and Khobi folds show evidence of crestal erosion during the fold growth (Figure 5B). Seismic reflection profile R-16 imaging onlaps within the growth sequences (Figure 5B). Pliocene strata above the onlapping growth units of the forelimb of the Khobi anticline reflect a later phase of structural growth involving a component of limb rotation (Figure 5B).

On the R-16 seismic profile, the formation sequence of the Khobi and Kvaloni anticlines is fairly well-observed. Taking into account the geometry of separate horizons of Upper Miocene growth strata we suppose that initially, the Khobi anticline was formed (Figure 5B). On the back and forelimb of the Kvaloni anticline, lower horizons of Late Miocene growth-strata beds are onlapping the pre-growth beds (Figure 5B). In the forelimb, folded growth strata are observed as well (Figure 5B). In contrast to the Khobi anticline, the Late Miocene growth strata structures in the backlimb of the Kvaloni anticline are represented by younger horizons (Figure 5B). These are the data which allow us to link the anticlines formation with the break-back thrust sequence.

In the cross-section construction, balancing, and restoration, some assumptions were made. One of the general problems in constructing a balanced cross-section is

"filling space" between a known detachment horizon at depth and the structural elevation of the sedimentary rocks exposed at the surface (e.g., Woodward et al., 1989). Although there are no duplexes exposed at the surface of the RFFTB, the balanced cross-sections suggest that Early-Middle Jurassic rocks could be duplexed in the subsurface. These duplexes fill space between the master detachment and the rocks exposed at the surface. The duplexes also account for the folding of higher-level detachment horizons as shown in the seismic profile and balanced cross-section (Figure 4B, 6A). The balanced cross-section show that the anticlines are developed above the location of the upper detachment level and that the thrust faults are the main control of the fault-propagation folding that formed the anticlines. The anticlines are mainly represented by south-vergent and north-vergent fault-propagation folds (Figure 6A). The balanced cross-section shows that the south-vergent duplexes are developed above the lower detachment level. The flat upper detachment is deformed by deeply rooted duplexes, associated with prominent fault-bend folds (Figure 6A). The frontal part of the RFFTB is represented by Chaladidi-Sagvamichao, Kvaloni, and Khobi anticlines. Chaladidi-Sagvamichao, Kvaloni, Khobi, Nokalakevi, Tsaishi, Sashurgaio, and Surakoni anticlines are interpreted as fault-propagation folds.

Seismic profile R-15 (Figure 4B) reveals the occurrence of normal faults within sedimentary strata. These faults are inherited from the Middle Jurassic-Middle Eocene and related to phases of extension. Most of them were not drawn in the balanced cross-section (Figure 6A) since they had no influence on the mechanics of the foreland fold-and-thrust belt.

Discussion

The discussion focuses on two topics: 1) deformation structural style and 2) defining the types of thrust-top basins in the RFFTB developed using the end-member modes of thrust sequences (e.g., Boyer and Elliott, 1982; Butler, 1982; Butler, 1987; Morley, 1988; McClay, 1992; Storti et al., 2000).

The regional balanced cross-section (Figure 6A) shows the general styles of deformations along the RFFTB and interpreted structural geometries which significantly differ from prior transects (e.g., Banks et al., 1997; Cowgill et al., 2016; Tari et al., 2018). Previous studies within the RFFTB indicate that compressional structures developed above the main detachment level and structures are represented by ramp anticlines or fault-related folds (Banks et al., 1997; Cowgill et al., 2016; Trexler et al., 2022). The main style of deformation within the RFFTB is represented by a set of growth fault-propagation folds, duplexes, and triangle zone (Figure 6A). The balanced cross-section (Figure 6A) reveals that the
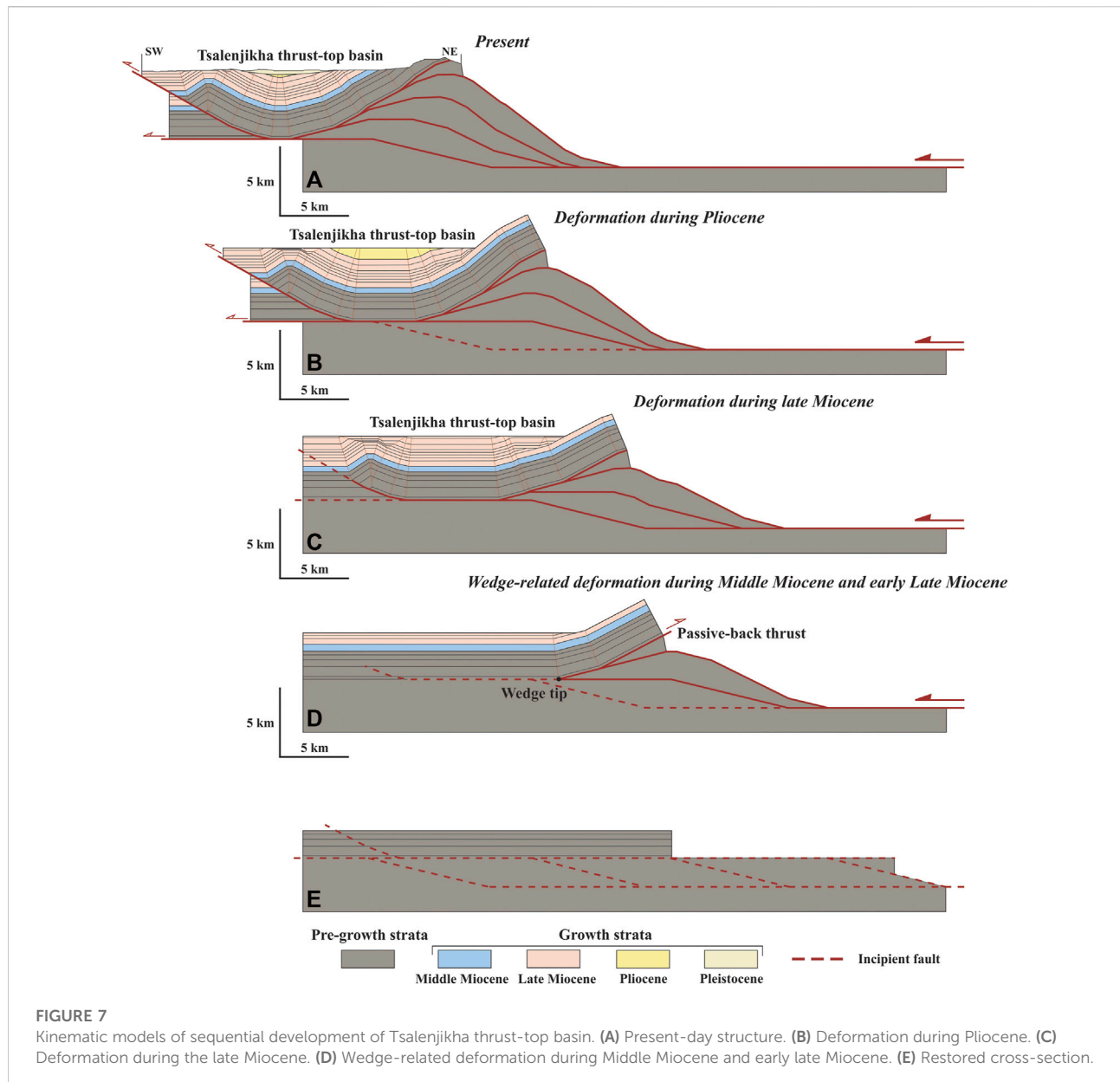
structure between the Khobi and Tsaishi anticlines is characterized by a ramp-dominated triangle zone and is represented by south-vergent duplexes and north-and south-vergent thrusts. The formation of these structure zone is similar to the classical model of triangle zone - Type-II (e.g., MacKay et al., 1996; Hagke and Malz, 2018).

The thin-skinned RFFTB is characterized by two major detachment levels. Two detachment levels that join on the termination of the duplexes developed under the Tsaishi anticline are well-observed on the interpreted seismic profile R-15 (Figure 4B). A balanced section restoration of compressional structures across the profile (A-A^1) provides a minimum estimate of shortening of -40%, equivalent -42.78 km (Figures 6A,B). Unfortunately, the estimation of the shortening value of the RFFTB was not carried out in previous studies. The shortening value was detected only for the Tsaishi anticline—5.3 km (Trexler et al., 2022).

The synclines within the RFFTB are filled by the Middle Miocene-Pleistocene shallow marine and continental syn-tectonic sediments, forming a series of typical thrust-top basins (e.g., Turner, 1988; Turner, 1990) associated with fault-propagation folds (Figure 6A). Thrust-top basins (or piggyback, wedge-top) are special among sedimentary basins in that they experience contraction during sedimentation and are a common feature in foreland basins systems worldwide (Turner, 1988; Butler and Grasso, 1993; DeCelles and Giles, 1996). The terms "thrust-top", "piggyback" or "wedge-top" basins were used for basins developed on active thrust sheets (Ori and Friend, 1984; Turner, 1988; Butler and Grasso, 1993; DeCelles and Giles, 1996). These terms that are used today in the geological literature often lead to misunderstandings. Our study area is not an exception. For instance, the Odishi piggyback basin (Banks et al., 1997), as well as the Rioni wedge-top basin (Forte et al., 2014), was distinguished and studied within the RFFTB.

One of the critical issues in the analysis of fold-and-thrust belts is the timing of thrusting. Several models have been proposed to explain deformation. These are: 1) a piggyback thrust sequence or a foreland-directed thrusting, where displacement is transferred onto a new thrust initiated in the footwall of the previously active thrust (Boyer and Elliott, 1982; Butler, 1982); 2) a break-back thrust sequence or a hinterland-directed thrusting, where new thrusts originate in the hangingwalls of older thrusts (Butler, 1987); 3) In-sequence thrusting, where a thrust sequence has formed progressively in one direction, which can either be a piggyback or a break-back sequence (McClay, 1992); 4) Out-of-sequence thrusting, where the sequence of thrusting does not conform with either a progressive piggyback or break-back sequence (Morley, 1988; McClay, 1992); and 5) Synchronous thrusting, where two or more thrusts accumulate displacement at the same time (Boyer, 1992; Storti et al., 2000). According to Storti et al. (2000),

FIGURE 7
Kinematic models of sequential development of Tsalenjikha thrust-top basin. **(A)** Present-day structure. **(B)** Deformation during Pliocene. **(C)** Deformation during the late Miocene. **(D)** Wedge-related deformation during Middle Miocene and early late Miocene. **(E)** Restored cross-section.
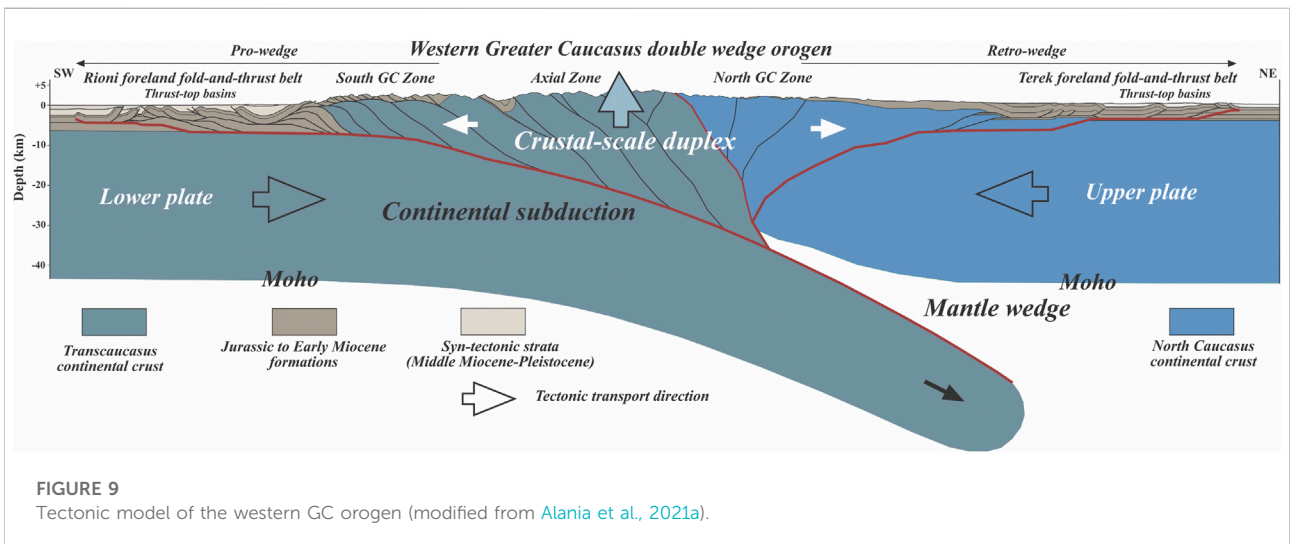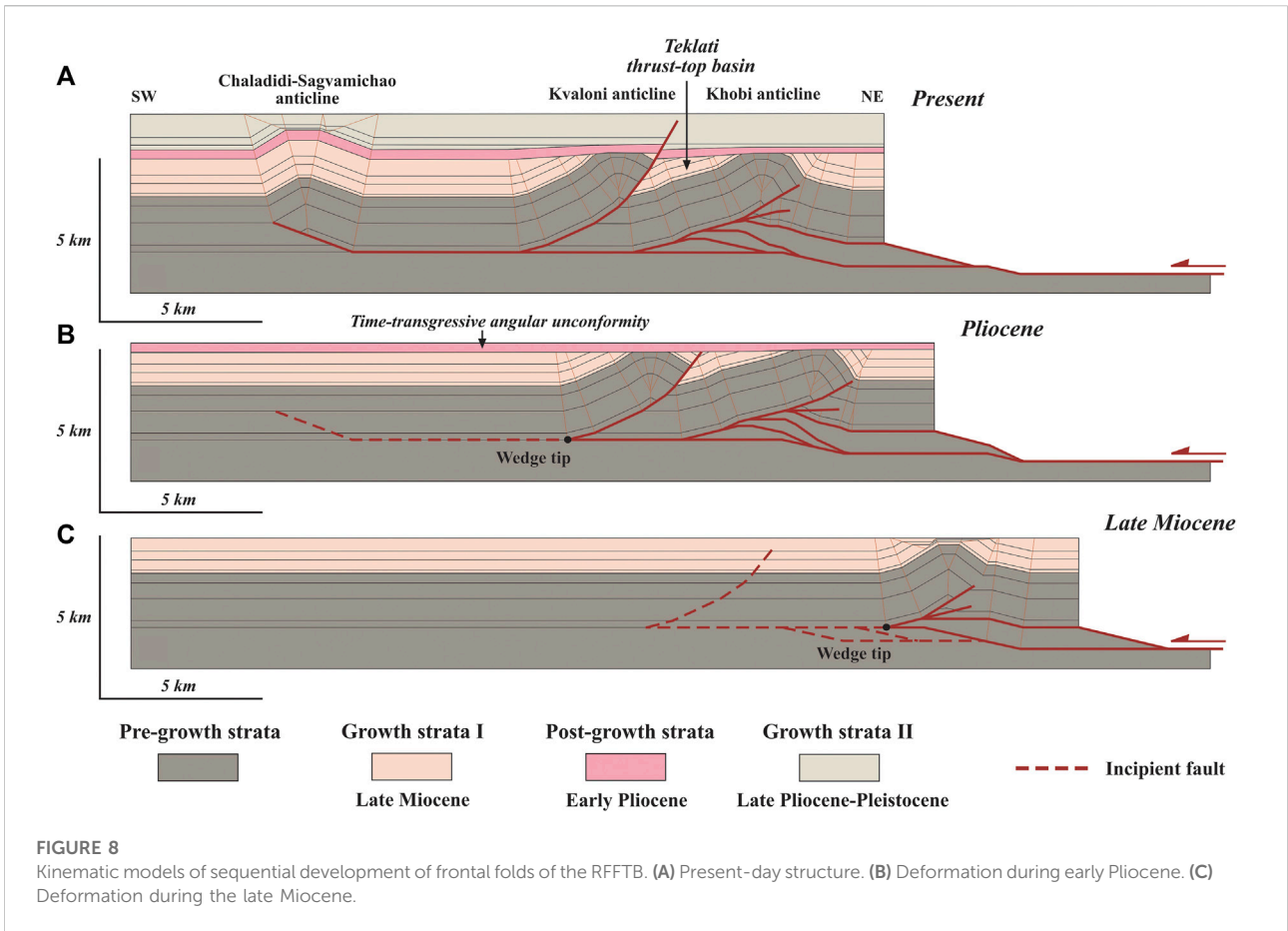
several of the above thrust sequence modes can act at the same time. The balanced cross-section (Figure 6A) shows that the sequence of thrusting in the RFFTB occurs mainly in two ways: a piggyback sequence (foreland-directed) and a break-back sequence (hinterland-directed). Fault-propagation folds and duplex structures formed the main structure of the RFFTB. The south-and north vergent fault-propagation folds are forming the thrust-top basins. The regional balanced cross-section (Figure 6A) shows that fault-propagation folds above the upper detachment level can develop by piggyback and break-back thrust sequences. The formation of fault-bend fold duplex structures above the lower detachment is related to piggyback thrust sequences

and is interpreted as a blind duplex (Figure 6A). The rejuvenation of thrust-top basins in the north-south direction is observed on the balanced cross-section (Figure 6A). Seven thrust-top basins have been defined within the study area. Chronologically, the oldest is the Tsalenjikha thrust-top basin, the formation of which began in the middle Miocene, and the youngest is the Sagvamichao basin (Pliocene-Pleistocene) (Figure 6A).

According to the definition of the piggyback basin (or thrust-top) by Ori and Friend (1984), it is formed and filled while being carried piggyback thrust sequence on active thrust sheets. Accordingly, we considered it appropriate to name the thrust-top basins related to break-back thrust sequences

FIGURE 8
Kinematic models of sequential development of frontal folds of the RFFTB. **(A)** Present-day structure. **(B)** Deformation during early Pliocene. **(C)** Deformation during the late Miocene.

FIGURE 9
Tectonic model of the western GC orogen (modified from Alania et al., 2021a).

break-back basins. Using end-member modes of thrust sequences (e.g., Butler, 1982; Butler, 1987; McClay, 1992) we can define three types of thrust-top basin: 1) Type

I-piggyback basin—the evolution of thrust-top basins was mainly controlled by the piggyback thrust sequence; 2) Type II-break-back basin (Teklati basin)—the evolution of

thrust-top basins was controlled by the break-back thrust sequence; and 3) Type III (Sagvamichao, Tsalenjikha basins)—formation of thrust-top basin is related to combined, piggyback and piggyback back thrust sequences and has bi-vergent geometry (Figure 6A). The majority of basins represent Type I (piggyback basin) and are developed between the growth fault-propagation folds (Narazeni, Nokalakhevi, and Dikhazungi basins). The Teklati basin represents the Type II (break-back basin) and is developed between the fault-propagation folds of Kvaloni and Khobi. The Sagvamichao and Tsalenjikha basins are characterized by bi-vergent geometry and are attributed to Type III (Figure 6A). The Sagvamichao basin is located between the south- and north-vergent growth fault-propagation folds. The geometry of the northern part of the wide Tsalenjikha thrust-top basin developed between the Sarakoni anticline and frontal monocline zone of the GC Southern Slope was controlled by duplex staking kinematics (Figures 6A, 7). The similar picture is typical for the Jaca basin in the South Pyrenean thrust-top basin (e.g., Turner, 1988). Since the Miocene the basin depocenters migration from the North to the South took place synchronously with the duplexes formation (Figure 7).

Kinematic models of sequential development of frontal folds of the RFFTB demonstrate that the formation of Chaladidi-Sagvamichao, Kvaloni, and Khobi anticline during Late Miocene-Pleistocene is related to combined thrust sequences (Figure 8).

According to Banks et al. (1997), the timing of the onset of Cenozoic deformation in the RFFTB is in the Late Miocene. Based on fission-track data, the exhumation process in the western GC started at the end of the Oligocene and reached its peak in the Pliocene-Pleistocene (Vincent et al., 2007; Avdeev and Niemi, 2011; Vincent et al., 2011). The geometry of syn-orogenic sedimentation, associated with footwall synclines and the sedimentary infill of thrust-top basins, provides information on the thrusting activity within the RFFTB (Figures 7, 8). From the Miocene times onward, the compressional deformation within pro-wedge foreland basin and the onset of Middle Miocene syn-tectonic sedimentation took place (Alania et al., 2021a). Within the RFFTB are distinguished three major changes in basin-fill dynamics: 1) marine/regressive stage (Middle Miocene-Early Pliocene), 2) marine/transgressive stage (Late Pliocene), and 3) marine-continental/transgressive-regressive cycle (Pleistocene-Holocene) (Jones and Simmons, 1997). Unfortunately, the study area lacks any detailed sedimentological studies of syntectonic strata, although the basin-fill dynamics could be reconstructed taking into account basin geometry and depositional conditions.

The tectonic model across the western GC (Figure 9) demonstrates that the retro-wedge and the Terek foreland basin developed on the upper plate, whereas the pro-wedge and the Rioni foreland basin developed on the lower,

subducting plate. According to Alania et al. (2021a), the build-up of the GC orogen is related to a two-phase compressive deformation: 1) an early, symmetric inversion during the Oligocene-Early Miocene, and 2) the formation of an asymmetric, double-wedge structure during the Middle Miocene-Pleistocene. Building of structures of the RFFTB was governed by the GC basement crustal-scale duplexes propagation along detachment horizons within the cover-generating thin-skinned structures made up of pre- (Jurassic, Cretaceous, Paleogene) and syn-orogenic (Miocene-Pleistocene) sequences (Figure 9).

The RFFTB is an excellent example of the formation of thrust-top basins related to piggyback, and break-back thrust sequences. Future integrated up-to-date sedimentological and thermochronological studies are fairly essential in order to strengthen the proposed structural model.

Conclusion

In this paper, we introduce the study results of the deformation structural style of the RFFTB using a seismic reflection profiles and a regional balanced cross-section. Our conclusions are summarized as follows:

- The main style of deformation within the thin-skinned RFFTB is represented by a set of growth fault-propagation folds, triangle zone, duplexes, and a series of thrust-top basins. The RFFTB is characterized by two major detachment levels. Fault-propagation folds above the upper detachments level can develop by piggyback and break-back thrust sequences. Duplex structures above the lower detachment can develop by piggyback thrust sequences.

- The amount of shortening obtained for this part of the regional balanced cross-section is 40% (−42.78 km).

- Within the RFFTB, a series of thrust-top basins developed. Fault-propagation folds and duplex structures formed the main structure of the thrust-top basins. The evolution of the thrust-top basins was mainly controlled by the kinematics of thrust sequences and competing growth fault-propagation folds. Using end-member modes of thrust sequences, the thrust-top basins are divided into: 1) Type I-piggyback basin, 2) Type II-break-back basin, and 3) Type III—formation of thrust-top basin characterized by bi-vergent geometry and related to combined, piggyback and piggyback back thrust sequences.

- Building of compressional structures of the RFFTB was governed by the GC basement crustal-scale duplexes propagation along detachment horizons within the cover-generating thin-skinned structures.

Data availability statement

The original contributions presented in the study are included in the article/Supplementary Material, further inquiries can be directed to the corresponding author.

Author contributions

VA: Conceptualization, Data acquisition, Data curation, Investigation, Methodology, Resources, Supervision, Validation, Visualization, Writing—original draft, editing. GM: Data curation, Investigation, Supervision, Methodology, Validation, Writing—original draft. PP: Methodology, Investigation, Validation, Writing—review and editing. IF: Investigation, Resources, Writing—review and editing. TB: Resources, Validation, Writing—review and editing. OE: Data curation, Investigation, Resources, Validation. AG: Investigation, Resources, Validation. AR: Investigation, Resources, Validation.

Funding

Acknowledgments

Conflict of interest

The authors declare that the research was conducted in the absence of any commercial or financial relationships that could be construed as a potential conflict of interest.

Publisher's note

All claims expressed in this article are solely those of the authors and do not necessarily represent those of their affiliated organizations, or those of the publisher, the editors and the reviewers. Any product that may be evaluated in this article, or claim that may be made by its manufacturer, is not guaranteed or endorsed by the publisher.

References

Adamia, S., Alania, V., Tsereteli, N., Varazanashvili, O., Sadradze, N., Lursmanashvili, N., et al. (2017). Postcollisional tectonics and seismicity of Georgia. *GSA Spec. Pap.* 525, 535–572. doi:10.1130/2017.2525(17

Adamia, Sh., Alania, V., Chabukiani, A., Chichua, G., Enukidze, O., and Sadradze, N. (2010). Evolution of the late cenozoic basins of Georgia (SW Caucasus): A review. *Geol. Soc. Lond. Spec. Publ.* 340, 239–259. doi:10.1144/SP340.11

Adamia, S. H., Alania, V., Chabukiani, A., Kutelia, Z., and Sadradze, N. (2011b). Great Caucasus (cavcasioni): A long-lived north-tethyan back-arc basin. *Turkish J. Earth Sci.* 20, 611–628. doi:10.3906/yer-1005-12

Adamia, Sh., Alania, V., Chabukiani, A., Maisuradze, G., and Kuloshvili, S. (2004). "Seismic source zone models of recent earthquakes of Georgia," in *Proceedings of the 5th international symposium on eastern mediterranean Geology.* Editors A. A. Chatzipetros and S. B. Pavlides (Thessaloniki, Greece: International Symposium on Eastern Mediterranean Geology), 545–551.

Adamia, Sh., Chkhotua, T., Kekelia, M., Lordkipanidze, M., Shavishvili, I., and Zakariadze, G. (1981). Tectonics of the Caucasus and adjoining regions: Implications for the evolution of the tethys ocean. *J. Struct. Geol.* 3, 437–447. doi:10.1016/0191-8141(81)90043-2

Adamia, Sh., Sadradze, N., Alania, V., Talakhadze, G., and Khmaladze, K. (2020). *Geology of lithosphere of the Georgia, deep structure, geodynamics and evolution.* Georgia: Tbilisi State University, Diagrama Press.

Adamia, S. H., Zakariadze, G., Chkhotua, T., Sadradze, N., Chabukiani, A., Gventsadze, A., et al. (2011a). Geology of the Caucasus: A review. *Turkish J. Earth Sci.* 20, 489–544. doi:10.3906/yer-1005-11

Alania, V., Beridze, T., Enukidze, O., Chagelishvili, R., Lebanidze, Z., Maqadze, D., et al. (2021b). "The geometry of the two orogens convergence and collision zones in Central Georgia: New data from seismic reflection profiles," in *Building knowledge for geohazard assessment and management in the Caucasus and other orogenic regions.* Editors F. L. Bonali, F. Pasquaré Mariotto, and N. Tsereteli (Dordrecht: Springer, NATO Science

for Peace and Security Series C: Environmental Security), 73–88. doi:10.1007/978-94-024-2046-3_6

Alania, V., Chabukiani, A., Chagelishvili, R., Enukidze, O., Gogrichiani, K., Razmadze, A., et al. (2017). Growth structures, piggy-back basins and growth strata of the Georgian part of the Kura foreland fold–thrust belt: Implications for late alpine kinematic evolution. *Geol. Soc. Lond. Spec. Publ.* 428, 171–185. doi:10.1144/SP428.5

Alania, V., Pace, P., Corrado, S., Gusmeo, T., Beridze, T., Sadradze, N., et al. (2021c). Preliminary structural interpretation of a seismic profile across the frontal sector of the eastern achara-Trialeti fold-and-Thrust belt. *Bull. Georg. Natl. Acad. Sci.* 15, 74–80.

Alania, V., Tibaldi, A., Bonali, F., Enukidze, O., and Russo, E. (2021a). "Structural architecture of the Western Greater Caucasus orogen: New data from a crustal-scale structural cross-section," in *Building knowledge for geohazard assessment and management in the Caucasus and other orogenic regions.* Editors F. L. Bonali, F. Pasquaré Mariotto, and N. Tsereteli (Dordrecht: Springer, NATO Science for Peace and Security Series C: Environmental Security), 59–71. doi:10.1007/978-94-024-2046-3_5

Avdeev, B., and Niemi, N. A. (2011). Rapid Pliocene exhumation of the central Greater Caucasus constrained by low-temperature thermochronometry. *Tectonics* 30, TC2009. doi:10.1029/2010TC002808

Banks, C. J., Robinson, A. G., and Williams, M. P. (1997). "Structure and regional tectonics of the Achara-Trialet fold belt and the adjacent Rioni and Kartli foreland basins, Republic of Georgia," in *Regional and petroleum Geology of the black sea and surrounding region.* Editor A. G. Robinson (Tulsa, OK, United States: American Association of Petroleum Geologists Memoir), 68, 331–346. doi:10.1306/M68612C17

Boyer, S. E., and Elliott, D. (1982). Thrust systems. *Am. Assoc. Pet. Geol. Bull.* 66, 1196–1230. doi:10.1306/03B5A77D-16D1-11D7-8645000102C1865D

Boyer, S. E. (1992). "Geometric evidence for synchronous thrusting in the southern Alberta and northwest Montana thrust belts," in *Thrust tectonics.* Editor K. R. McClay (Dordrecht, Netherlands: Springer), 377–390.

Brandes, C., and Tanner, D. C. (2014). fault-related folding: A review of kinematic models and their application. *Earth-Science Rev.* 138, 352–370. doi:10.1016/j.earscirev.2014.06.008

Butler, R. W. H., and Grasso, M. (1993). Tectonic controls on base-level variations and depositional sequences within thrust-top and foredeep basins: Examples from the neogene thrust belt of central sicily. *Basin Res.* 5, 137–151. doi:10.1111/j.1365-2117.1993.tb00062.x

Butler, R. W. H. (1982). The terminology of structures in thrust belts. *J. Struct. Geol.* 4, 239–245. doi:10.1016/0191-8141(82)90011-6

Butler, R. W. H. (1987). Thrust sequences. *J. Geol. Soc. Lond.* 144, 619–634. doi:10.1144/gsjgs.144.4.0619

Chanvry, E., Deschamps, R., Joseph, P., Puigdefàbregas, C., Poyatos-Moré, M., Serra-Kiel, J., et al. (2018). The influence of intrabasinal tectonics in the stratigraphic evolution of piggyback basin fills: Towards a model from the Tremp-Graus-Ainsa Basin (South-Pyrenean Zone, Spain). *Sediment. Geol.* 377, 34–62. doi:10.1016/j.sedgeo.2018.09.007

Corrado, S., Gusmeo, T., Schito, A., Alania, V., Enukidze, O., Conventi, E., et al. (2021). Validating far-field deformation styles from the Adjara-Trialeti fold-and-thrust belt to the Greater Caucasus (Georgia) through multi-proxy thermal maturity datasets. *Mar. Pet. Geol.* 130, 105141. doi:10.1016/j.marpetgeo.2021.105141

Cowgill, E., Forte, A. M., Niemi, N., Avdeev, B., Tye, A., Trexler, C., et al. (2016). Relict basin closure and crustal shortening budgets during continental collision: An example from Caucasus sediment provenance. *Tectonics* 35, 2918–2947. doi:10.1002/2016TC004295

DeCelles, P. G., and Giles, K. A. (1996). Foreland basin systems. *Basin Res.* 8, 105–123. doi:10.1046/j.1365-2117.1996.01491.x

Forte, A. M., Cowgill, E. S., and Whipple, K. X. (2014). Transition from a singly vergent to doubly vergent wedge in a young orogen: The Greater Caucasus. *Tectonics* 33, 2077–2101. doi:10.1002/2014TC003651

Gusmeo, T., Andrea, C., Corrado, S., Alania, V., Enukidze, O., Massimiliano, Z., et al. (2022). Tectono-thermal evolution of central Transcaucasia: Thermal modelling, seismic interpretation, and low-temperature thermochronology of the eastern Adjara-Trialeti and Western Kura sedimentary basins (Georgia). *J. Asian Earth Sci.* 238, 105355. doi:10.1016/j.jseaes.2022.105355

Gusmeo, T., Cavazza, C., Alania, V., Enukidze, O., Zattin, M., and Corrado, S. (2021). Structural inversion of back-arc basins-The Neogene Adjara-Trialeti fold-and-thrust belt (SW Georgia) as a far-field effect of the Arabia-Eurasia collision. *Tectonophysics* 803, 228702. doi:10.1016/j.tecto.2020.228702

Hagke, C., and Malz, A. (2018). Triangle zones - geometry, kinematics, mechanics, and the need for appreciation of uncertainties. *Earth-Science Rev.* 177, 24–42. doi:10.1016/j.earscirev.2017.11.003

Heydarzadeh, K., BrunoRuh, J., Vergés, J., Hajialibeigi, H., and Gharabeigi, G. (2020). Evolution of a structural basin: Numerical modelling applied to the dehdasht basin, central zagros, Iran. *J. Asian Earth Sci.* 187, 104088. doi:10.1016/j.jseaes.2019.104088

Jabbour, M., Dhont, D., Hervouët, Y., and Deroin, J. (2012). Geometry and kinematics of fault-propagation folds with variable interlimb angle. *J. Struct. Geol.* 42, 212–226. doi:10.1016/j.jsg.2012.05.002

Janelidze, A., and Kandelaki, N. (1956). *Geological map of the USSR, Caucasus series sheet K-38-XIII*. Moscow: Ministry of Geology.

Jones, R. W., and Simmons, M. D. (1997). "A review of the stratigraphy of eastern paratethys (Oligocene—holocene), with particular emphasis on the black sea," in *Regional and petroleum Geology of the black sea and surrounding region*. Editor A. G. Robinson (Tulsa, OK, United States: American Association of Petroleum Geologists Memoir), 68, 39–52. doi:10.1306/M68612C4

MacKay, P. A., Varsek, J. L., Kubli, T. E., Dechesne, R. G., Newson, A. C., and Reid, J. P. (1996). Triangle zones and tectonic wedges: An introduction. *Bull. Can. Pet. Geol.* 44, 1–5.

Mayer, J., Sachsenhofer, R. F., Ungureanu, C., Tari, G., Gratzer, R., Sweda, M., et al. (2018). Petroleum charge and migration in the black sea: Insights from oil and source rock geochemistry. *J. Petroleum Geol.* 41, 337–350. doi:10.1111/jpg.12706

McClay, K. R. (1992). "Glossary of thrust tectonics terms," in *Thrust tectonics*. Editor K. R. McClay (Dordrecht, Netherlands: Springer), 419–433.

Medwedeff, D. A. (1990). "Geometry and kinematics of an active, laterally propagating wedge thrust, wheeler ridge," in *Geometry and kinematics of an active, laterally propagating wedge thrust, wheeler ridge, California*. Editors S. Mitra and G. Fisher (California: The Johns Hopkins University Press), 3–28.

Melikadze, G., Kapanadze, N., Kobzev, G., Jimsheladze, T., and Sborshchikov, A. (2014). Assessment of the geothermal potential of West Georgia. *Nano Stud.* 50 (44), 123–128.

Morley, C. K. (1988). Out-of-sequence thrusts. *Tectonics* 7, 539–561. doi:10.1029/TC007i003p00539

Mosar, J., Kangarli, T., Bochud, M., Glasmacher, U. A., Rast, A., Brunet, M. F., et al. (2010). Cenozoic–Recent tectonics and uplift in the greater Caucasus: A perspective from Azerbaijan. *Geol. Soc. Lond. Spec. Publ.* 340, 261–280. doi:10.1144/sp340.12

Mosar, J., Mauvilly, J., Koiava, K., Gamkrelidze, I., Enna, N., Lavrishev, V., et al. (2022). Tectonics in the Greater Caucasus (Georgia – Russia): From an intracontinental rifted basin to a doubly verging fold-and-thrust belt. *Mar. Pet. Geol.* 140, 105630. doi:10.1016/j.marpetgeo.2022.105630

Nemcok, M., Glonti, B., Yukler, A., and Marton, B. (2013). Development history of the foreland plate trapped between two converging orogens: Kura Valley, Georgia, case study. *Geol. Soc. Lond. Spec. Publ.* 377, 159–188. doi:10.1144/SP377.9

Ori, G. G., and Friend, P. (1984). Sedimentary basins formed and carried piggyback on active thrust sheets. *Geol.* 12, 475–478. doi:10.1130/0091-7613(1984)12<475:sbfacp>2.0.co;2

Sachsenhofer, R., Popov, V., Bechtel, A., Coric, S., Francu, J., Gratzer, R., et al. (2018). Oligocene and lower Miocene source rocks in the paratethys: Palaeogeographical and stratigraphic controls. *Geol. Soc. Lond. Spec. Publ.* 464, 267–306. doi:10.1144/SP464.1

Shaw, J. H., Connors, C. D., and Suppe, J. (2005). Seismic interpretation of contractional fault-related folds. *AAPG Stud. Geol.* 53. doi:10.1306/St531003

Sobornov, K. O. (1996). Lateral variations in structural styles of tectonic wedging in the northeastern Caucasus, Russia. Bull. *Can. Petr. Geol.* 44, 385–399. doi:10.35767/gscpgbull.44.2.385

Sokhadze, G., Floyd, M., Godoladze, T., King, R., Cowgill, E. S., Javakhishvili, Z., et al. (2018). Active convergence between the lesser and greater Caucasus in Georgia: Constraints on the tectonic evolution of the lesser-greater Caucasus continental collision. *Earth Planet. Sci. Lett.* 481, 154–161. doi:10.1016/j.epsl.2017.10.007

Sosson, M., Stephenson, S., Sheremet, Y., Rolland, Y., Adamia, Sh., Melkonian, R., et al. (2016). The eastern Black Sea-Caucasus region during the Cretaceous: New evidence to constrain its tectonic evolution. *Comptes Rendus Geosci.* 348, 23–32. doi:10.1016/j.crte.2015.11.002

Storti, F., Salvini, F., and McClay, K. (2000). Synchronous and velocity-partitioned thrusting and thrust polarity reversal in experimentally produced, doubly-vergent thrust wedges: Implications for natural orogens. *Tectonics* 19, 378–396. doi:10.1029/1998TC001079

Suppe, J., Chou, G. T., and Hook, S. C. (1992). "Rates of folding and faulting determined from growth strata," in *Thrust tectonics*. Editor K. R. McClay (Dordrecht, Netherlands: Springer), 105–121. doi:10.1007/97894-011-3066-0_9

Suppe, J., and Medwedeff, D. A. (1990). Geometry and kinematics of fault-propagation folding. *Eclogae Geol. Helv.* 83, 409–454.

Suriano, J., Limarino, C. O., Tedesco, A. M., and Alonso, M. S. (2015). Sedimentation model of piggyback basins: Cenozoic examples of san juan precordillera, Argentina. *Geol. Soc. Lond. Spec. Publ.* 399, 221–244. doi:10.1144/SP399.17

Tari, G., Vakhania, D., Tatishvili, G., Mikeladze, V., Gogritchiani, K., Vacharadze, S., et al. (2018). "Stratigraphy, structure and petroleum exploration play types of the Rioni Basin, Georgia," in *Petroleum Geology of the black sea*. Editors M. Simmons, G. Tari, and I. Okay (London, United Kingdom: Geol. Soc. Lond), 464, 403–438. Spec. Publications. doi:10.1144/SP464.14

Tari, G., Vrsic, A., Gumpenberger, T., Mekonnen, E., Hujer, W., Fallah, M., et al. (2021). Eocene volcaniclastics in the kartli basin, Georgia: A fractured reservoir sequence. *J. Petroleum Geol.* 44 (3), 413–433. doi:10.1111/jpg.12795

Tibaldi, A., Alania, V., Bonali, F., Enukidze, O., Tsereteli, N., Kvavadze, N., et al. (2017a). Active inversion tectonics, simple shear folding and back-thrusting at Rioni Basin, Georgia. *J. Struct. Geol.* 96, 35–53. doi:10.1016/j.jsg.2017.01.005

Tibaldi, A., Bonali, F. L., Russo, E., and Pasquarè Mariotto, F. A. (2018). Structural development and stress evolution of an arcuate fold-and-thrust system, southwestern Greater Caucasus, Republic of Georgia. *J. Asian Earth Sci.* 156, 226–245. doi:10.1016/j.jseaes.2018.01.025

Tibaldi, A., Russo, E., Bonali, F. L., Alania, V., Chabukiani, A., Enukidze, O., et al. (2017b). 3-D anatomy of an active Fault-propagation fold: A multidisciplinary case study from Tsaishi, Western Caucasus (Georgia). *Tectonophysics* 717, 253–269. doi:10.1016/j.tecto.2017.08.006

Tibaldi, A., Tsereteli, N., Varazanashvili, O., Babayev, G., Barth, A., Mumladze, T., et al. (2020). Active stress field and fault kinematics of the Greater Caucasus. *J. Asian Earth Sci.* 188, 104108. doi:10.1016/j.jseaes.2019.104108

Trexler, C. C., Cowgill, E., Spencer, J. Q. G., and Godoladze, T. (2020). Rate of active shortening across the southern thrust front of the Greater Caucasus in Western Georgia from kinematic modeling of folded river terraces above a listric thrust. *Earth Planet. Sci. Lett.* 544, 116362. doi:10.1016/j.epsl.2020.116362

Trexler, C., Cowgill, E., Niemi, N., Vasey, D., and Godoladze, T. (2022). Tectonostratigraphy and major structures of the Georgian Greater Caucasus: Implications for structural architecture, along-strike continuity, and orogen evolution. *Geosphere* 18, 211–240. doi:10.1130/GES02385.1

Tsereteli, N., Tibaldi, A., Alania, V., Gventsadse, A., Enukidze, O., Varazanashvili, O., et al. (2016). Active tectonics of central-Western Caucasus, Georgia. *Tectonophysics* 691, 328–344. doi:10.1016/j.tecto.2016.10.025

Turner, J. P. (1990). Structural and stratigraphic evolution of the West Jaca thrust-top basin, Spanish Pyrenees. *J. Geol. Soc. Lond.* 147, 177–184. doi:10.1144/gsjgs.147.1.0177

Turner, J. P. (1988). "Tectonic and stratigraphic evolution of the West Jaca thrust-top basin, southwestern Pyrenees," (Bristol, England: University of Bristol). Ph.D. thesis.

Vakhania, D. (2008a). General overview of gas and oil saturation of sedimentary cover of the West (Kolkhida) zone of the sinking Transcaucasian intermountain region against the background of oil and gas generation problems. *Georgian Oil Gas* 22, 87–107.

Vakhania, D. (2008b). Geodynamic evolution of oil and gas deposit generation within the Western (Kolkhida) zone of the sinking Transcaucasian intermountain region. *Georgian Oil Gas* 22, 108–130.

Vincent, S. J., Braham, W., Lavrishchev, V. A., Maynard, J. R., and Harland, M. (2016). the formation and inversion of the Western greater Caucasus basin and the uplift of the Western greater Caucasus: Implications for the wider black sea region. *Tectonics* 35, 2948–2962. doi:10.1002/2016TC004204

Vincent, S. J., Carter, A., Lavrishchev, V. A., Rice, S. P., Barabadze, T. G., and Hovius, N. (2011). The exhumation of the Western greater Caucasus: A thermochronometric study. *Geol. Mag.* 148 (1), 1–21. doi:10.1017/S0016756810000257

Vincent, S. J., Morton, A. C., Carter, A., Gibbs, S., and Barabadze, T. G. (2007). Oligocene uplift of the western greater Caucasus: An effect of initial arabia-eurasia collision. *Terra nova.* 19, 160–166. doi:10.1111/j.1365-3121.2007.00731.x

Woodward, N. B., Boyer, S. E., and Suppe, J. (1989). *Balanced geological cross-sections: An essential technique in geological research and exploration*, 6. Washington, D. C: AGU. Short Course Geol.